Phenomenology of summer ozone episodes over the Madrid Metropolitan Area, central Spain

Querol X.[1], Alastuey A.[1], Gangoiti G. [2], Perez N.[1], Lee H.K.[3], Eun H.R.[3], Park H.Y.[3], Mantilla E.[4], Escudero M.[5], Titos G.[1], Alonso L.[2], Temime-Roussel B.[6], Marchand N.[6], Moreta J.R[7], Revuelta M.A.[7], Salvador P.[8], Artíñano B.[8], García dos Santos S.[9], Anguas M.[10], Notario A.[11], Saiz-Lopez A.[10], Harrison R.M.[12], Ahn K.-H.[3]

[1]Institute of Environmental Assessment and Water Research (IDAEA-CSIC), C/Jordi Girona 18-26, Barcelona, 08034 Spain

[2]Escuela Técnica Superior Ingeniería de Bilbao, Departamento Ingeniería Química y del Medio Ambiente, Universidad del País Vasco UPV/EHU, Urkixo Zumarkalea, S/N, Bilbao, 48013 Spain

[3]Department of Mechanical Engineering, Hanyang University, Ansan 425-791, Republic of Korea

[4]Centro de Estudios Ambientales del Mediterráneo, CEAM, Unidad Asociada al CSIC, Parque Tecnológico C/ Charles R. Darwin, 14 Paterna, Valencia, 46980 Spain

[5] Centro Universitario de la Defensa de Zaragoza, Academia General Militar, Ctra. de Huesca s/n, Zaragoza, 50090 Spain

[6]Aix Marseille Univ, CNRS, LCE, Marseille, France

[7]Agencia Estatal de Meteorología, AEMET, C/ Leonardo Prieto Castro, 8, Madrid, 28071 Spain

[8]Department of Environment, CIEMAT, Joint Research Unit Atmospheric Pollution CIEMAT-CSIC, c/ Avenida Complutense 40, Madrid, 28040 Spain

[9]Centro Nacional de Sanidad Ambiental. Instituto de Salud Carlos III (ISCIII), Ctr Majadahoda a Pozuelo km 2, Majadahonda (Madrid), 28222 Spain

[10]Department of Atmospheric Chemistry and Climate, Institute of Physical Chemistry Rocasolano, CSIC, Madrid, 28006 Spain

[11]University of Castilla-La Mancha, Physical Chemistry Department, Faculty of Chemical Science and Technologies, Ciudad Real, Spain.

[12]National Centre for Atmospheric Science, University of Birmingham, B15 2TT United Kingdom. [+]Also at: Department of Environmental Sciences/Centre for Excellence in Environmental Studies, King Abdulaziz University, Jeddah, Saudi Arabia

SUPPLEMENTARY MATERIAL

PTRMS measurements and O_3 Formation Potential (OFP)

A PTR-TOF-MS8000 (Ionicon Analytik Ges.m.b.H., Innsbruck, Austria) operating in $H3O^+$ mode was deployed at the ISCIII site from 04 to 19/07/2016. Detailed description of the instrument can be found in Graus et al (2010). The reaction conditions were a drift voltage of 545 V, a chamber temperature of 60°C and a drift pressure of 2.2 mbar resulting in an E/N of about 120 td. The time resolution was 1 min. The mass resolution, as well as the mass accuracy and the relative transmission efficiency were routinely verified using a 12 compounds gas standard including aldehydes, ketones and aromatics from m/z 45 to m/z 181 (100 ppb each in Nitrogen). The data was treated using the Software 2.4.2 software (Ionicon Analytik Ges.m.b.H., Innsbruck, Austria). The mixing ratios in pbb$_v$ are calculated using the ratio between the signal of the individual ions C^+ and the signal of the reagent ion H_3O^+ taking into account the drift voltage (Udrift), drift temperature (Tact), drift pressure (pact) as well as the reaction rate of the ion with the H_3O^+ ion (k) and the transmission of the compound (TR_{C+}) relative to the transmission of the reagent ion (TR_{H3O+}). K value from Cappellin et al. (2012) were used for the concentration calculation, when available. Otherwise, the default value

(2.00x10^{-9} cm^3/s) was used. They are reported in table S1. Regarding formaldehyde, the water content correction procedure developed by Vlasenko et al (2010) was applied.

Ozone formation potential (OFP) were assessed on a basis of 24 VOCs or group of VOCs quantified (table S1), for which an unambiguous molecular identification can be inferred and a MIR (Maximum Incremental Reactivity) is available in the literature. The MIR scale is the incremental reactivity (IR) of a VOC computed for conditions in which the compound has its maximum absolute IR value (Carter, 1994). This generally occurs at a low VOC-to-NOx ratio in which the chemistry is VOC-limited. OFP corresponds thus to a maximum O$_3$ concentration formation for a VOC, or mix of VOCs (Carter, 1994). In this study, we used the updated MIR values from Carter (2009)(Table S1). For monoterpenes, a weighted MIR value has been calculated assuming a constant composition of 45% α-pinene, 18% β-pinene, 28% limonene, 7% myrcene and 2% camphene. These proportions were assessed from 2 Tenax cartridges analysis collected on 19/07/2016 at the ISCIII site. Total OFP (μg m^{-3}) as well as the relative contribution of the 24 VOCs or group of VOCs are reported in table S1 for 3 selected days: 06/07/2016 (accumulation day), 14/07/2016 (transition day) and 13/07/2016 (venting day). For each day, we considered 3 distinct periods: Morning traffic peak (06:00-09:00 UTC), maximum insolation/biogenic VOC emissions period (11:00- 13:00 UTC), and evening traffic peak (19:30-21:30 UTC). Average daytime OFP (06:00-21:30 UTC) for each selected days as well as overall campaign average are also reported in table S1 and figure S1.

It's important to consider that the OFP reported here represent only partial assessment of the overall OFP in the MMA. This analysis does not consider any alkanes nor alkenes which may be very significant OFP contributors in urban environments (Duan et al., 2008, for example). The PTR-ToF-MS can only measure compounds with proton affinity higher than that of water (about 697 kJ mol^{-1}) (Lindinger et al., 1998a, b), therefore compounds like methane (544 kJ mol^{-1}), ethane (596 kJ mol^{-1}), propane (626 kJ mol^{-1}), butane (678 kJ mol^{-1}), ethene (641 kJ mol^{-1}) and acetylene (641 kJ mol^{-1}) could not be detected. For higher molecular weight alkanes or alkenes the fragmentation patterns are not specific enough to allow a proper identification and quantification.

Due to higher VOC concentrations, OFP are significantly higher during the accumulation period (06/07/2016) than during the transition (14/07/2016) and venting (13/07/2016) days. However, the relative contributions of the different VOC families stay relatively constant whatever period is considered (Figure S1). The total OFP is largely dominated by the impact of carbonyls representing between 42 and 67% of the total OFP, and particularly by formaldehyde and acetaldehyde. Aromatics and oxygenated aromatics show more variability with higher contributions during the morning traffic peaks (up to 27% of the total OFC during accumulation periods). However, the impact of the morning traffic emissions is compensated, all along the day, by the emissions of biogenic VOCs (isoprene and monoterpenes) and the formation of their main oxidation products (methylglyoxal, methacrolein, methyl vinyl ketone) (Table S1), contributing up to 16% of the OFP. Accumulation periods favouring the formation of O$_3$ from VOCs emitted and formed within the MMA, this result highlights the potential importance of biogenic emissions towards the O$_3$ concentrations observed in a large urban area such as Madrid, whose relative contribution to the OFP will increase with the distance to urban areas. However, as carbonyls and alkanes/alkenes are largely emitted by anthropogenic sources (vehicular emissions, mostly) and/or significantly produced by the oxidation of

anthropogenic VOCs (for carbonyls), the anthropogenic emissions may still largely dominate the OFP. And because, it was not possible to include the, mostly anthropogenic, alkanes/alkenes in the OFP calculations the anthropogenic VOCs contribution to OFP should be considered as the minimum one.

References

Cappellin, L. et al., 2012. On Quantitative Determination of Volatile Organic Compound Concentrations Using Proton Transfer Reaction Time-of-Flight Mass Spectrometry, Environmental Science & Technology, 46, 2283-2290.
Carter, W. P. L., 1994. Development of Ozone Reactivity Scales for Volatile Organic Compounds, J. Air & Waste Manage. Assoc., 44, 881-899.
Carter, W. P. L., 2009. Updated Maximum incremental reactivity scale and hydrocarbon bin reactivities for regulatory applications. Available at
https://www.arb.ca.gov/research/reactivity/mir09.pdf (last access: 1 October 2017).
Duan, J., Tan J., Yang L., Wu S., Hao J., 2008. Concentration, sources and ozone formation potential of volatile organic compounds (VOCs) during ozone episode in Beijing, Atmospheric Research, 88, 1, 25-35.
Graus, M., Muller, M., Hansel, A., 2010. High Resolution PTR-TOF: Quantification and Formula Confirmation of VOC in Real Time, Journal of the American Society For Mass Spectrometry, 21, 1037-1044.
Lindinger, W., Hansel, A., Jordan, A., 1998a. On-line monitoring of volatile organic compounds at pptv levels by means of proton-transfer-reaction mass spectrometry (PTR-MS) - Medical applications, food control and environmental research, International Journal of Mass Spectrometry, 173, 191-241.
Lindinger, W., Hansel, A., Jordan, A., 1998b. Proton-transfer-reaction mass spectrometry (PTR-MS): on-line monitoring of volatile organic compounds at pptv levels, Chemical Society Reviews, 27, 347-354.
Vlasenko, A., Macdonald, A. M., Sjostedt, S. J., Abbatt, J. P. D., 2010. Formaldehyde measurements by Proton transfer reaction – Mass Spectrometry (PTR-MS): correction for humidity effects, Atmos. Meas. Tech., 3, 1055-1062.

Table S1. Ozone Formation Potential (OFP) and relative contribution of VOCs as measured by the PTR-ToF-MS (ISCIII site) to the total OFP. [1]MIR (Maximum Incremental Reactivity, µgO$_3$ per µgVOC) are from Carter (2009), [2] [VOC]xMIR, µg m^{-3}. PTR-MS doe s not allows measuring alkenes and alkanes (mostly anthropogenic) and accordingly these were not included in the OFP calculations.

m/z	k [10^{-9}cm3/s]	Most probable compounds	MIR [1]	06/07/2016 6-9h	11-13h	19h30-21h30	6-21h30	14/07/2016 6-9h	11-13h	19h30-21h30	6-21h30	13/07/2016 6-9h	11-13h	19h30-21h30	6-21h30	Avg Camp
		time UTC		6-9h	11-13h	19h30-21h30	6-21h30	6-9h	11-13h	19h30-21h30	6-21h30	6-9h	11-13h	19h30-21h30	6-21h30	
		OFP tot (µ/m^3)^2		299.3	193.9	211.4	199.1	87.6	85.3	83.8	96.6	77.9	92.0	80.8	94.0	155.4
		Most probable compounds MIR [1]		*Relative contribution*												
31.0178	2.00	Formaldehyde	9.24	20.5%	36.5%	32.5%	33.7%	39.5%	49.5%	43.3%	42.8%	45.6%	49.4%	47.1%	47.1%	35.5%
33.0335	2.14	Methanol	1.45	16.3%	12.8%	10.1%	12.7%	9.1%	9.1%	11.3%	8.9%	9.9%	10.0%	11.1%	9.7%	11.8%
45.0335	3.02	Acetaldehyde	6.34	12.1%	14.3%	16.0%	13.8%	12.6%	12.4%	9.5%	9.7%	12.1%	10.0%	9.9%	10.2%	14.7%
47.0128	1.99	Formic acid	0.062	0.1%	0.2%	0.1%	0.1%	0.1%	0.0%	0.0%	0.1%	0.1%	0.1%	0.1%	0.1%	0.1%
47.0491	2.18	Ethanol	1.25	0.5%	0.1%	0.5%	0.3%	0.7%	0.1%	0.6%	0.3%	0.8%	0.4%	1.0%	0.6%	0.6%
57.0335	3.05	Acrolein	7.24	1.6%	1.6%	1.5%	1.5%	1.8%	0.9%	0.6%	1.0%	1.6%	1.3%	1.5%	1.3%	1.4%
59.0491	3.32	Acétone	0.35	2.5%	3.1%	2.6%	2.9%	2.2%	2.5%	2.6%	2.4%	2.6%	2.8%	2.6%	2.7%	2.8%
61.0284	2.25	Acetic acid	0.66	2.2%	3.0%	2.6%	2.7%	2.0%	1.0%	0.8%	1.3%	2.2%	1.7%	1.1%	1.7%	2.4%
69.0699	1.96	Isoprene	10.28	4.1%	4.7%	4.2%	4.6%	3.9%	4.2%	7.2%	5.2%	4.5%	4.2%	6.2%	5.2%	4.7%
71.0491	3.05	Methacrolein/MVK	5.84	2.0%	3.4%	3.3%	2.8%	2.3%	4.5%	5.0%	4.0%	3.1%	2.7%	5.6%	3.7%	3.9%
73.0284	2.00	Methylglyoxal	16.02	3.9%	7.5%	5.2%	6.0%	0.5%	2.9%	0.7%	1.9%	2.4%	4.1%	2.8%	3.9%	5.1%
73.0648	3.28	Butanone	2	4.3%	1.6%	2.2%	2.3%	1.5%	1.1%	2.9%	1.6%	1.3%	1.4%	1.1%	1.4%	1.9%
75.0441	2.41	Methylacetate	0.067	0.0%	0.1%	0.1%	0.1%	0.0%	0.0%	0.0%	0.0%	0.0%	0.0%	0.0%	0.0%	0.1%
79.0542	1.93	Benzene	0.69	0.1%	0.1%	0.1%	0.1%	0.2%	0.1%	0.1%	0.1%	0.1%	0.1%	0.1%	0.1%	0.1%
87.0441	1.70	2.3 butanedione	2.61	0.8%	1.2%	1.0%	1.0%	0.4%	0.2%	0.1%	0.3%	0.5%	0.5%	0.3%	0.5%	0.8%
93.0699	2.08	toluene	3.88	9.2%	3.3%	7.5%	5.1%	2.9%	3.5%	6.9%	3.5%	3.1%	2.2%	2.5%	2.4%	4.8%
95.0491	2.18	phenol	2.69	0.1%	0.2%	0.2%	0.2%	0.1%	0.0%	0.0%	0.0%	0.1%	0.1%	0.1%	0.1%	0.1%
105.07	2.27	styrene	1.65	0.1%	0.1%	0.1%	0.1%	0.1%	0.0%	0.1%	0.1%	0.1%	0.0%	0.1%	0.1%	0.1%
107.049	3.82	benzaldehyde	-0.67	-0.1%	-0.1%	-0.1%	-0.1%	-0.1%	-0.1%	0.0%	-0.1%	-0.1%	-0.1%	-0.1%	-0.1%	-0.1%
107.086	2.26	C8 aromatics	7.48	14.2%	4.0%	6.8%	6.7%	11.7%	4.6%	4.7%	10.1%	6.2%	5.3%	3.4%	5.4%	5.6%
121.065	2.26	tolualdehyde	-0.59	-0.1%	0.0%	-0.1%	-0.1%	-0.1%	0.0%	0.0%	-0.1%	-0.1%	-0.1%	0.0%	-0.1%	-0.1%
121.101	2.41	C9 aromatics	5.65	2.9%	1.3%	2.3%	1.8%	6.4%	1.5%	1.6%	5.0%	1.4%	2.5%	1.4%	2.1%	1.9%
135.117	2.45	C10 aromatics	5.53	0.9%	0.4%	0.7%	0.6%	1.1%	0.4%	0.6%	0.7%	0.6%	0.4%	0.6%	0.5%	0.6%
137.132	2.43	monoterpenes	4.17	1.7%	0.8%	0.7%	1.0%	1.4%	1.1%	1.5%	1.2%	1.7%	0.9%	1.6%	1.4%	1.2%
		By family														
		Aromatics and O-Aromatics		27%	9%	18%	14%	22%	10%	14%	19%	11%	10%	8%	10%	13%
		Primary BVOCs		6%	5%	5%	6%	5%	5%	9%	6%	6%	5%	8%	7%	6%
		Secondary BVOCs		6%	11%	8%	9%	3%	7%	6%	6%	6%	7%	8%	8%	9%
		Total BVOC		*12%*	*16%*	*13%*	*14%*	*8%*	*13%*	*14%*	*12%*	*12%*	*12%*	*16%*	*14%*	*15%*
		Carbonyls (others)		42%	58%	56%	55%	58%	67%	59%	58%	64%	65%	63%	63%	57%
		Alcohol		17%	13%	11%	13%	10%	9%	12%	9%	11%	10%	12%	10%	12%
		Acids		2%	3%	3%	3%	2%	1%	1%	1%	2%	2%	1%	2%	2%
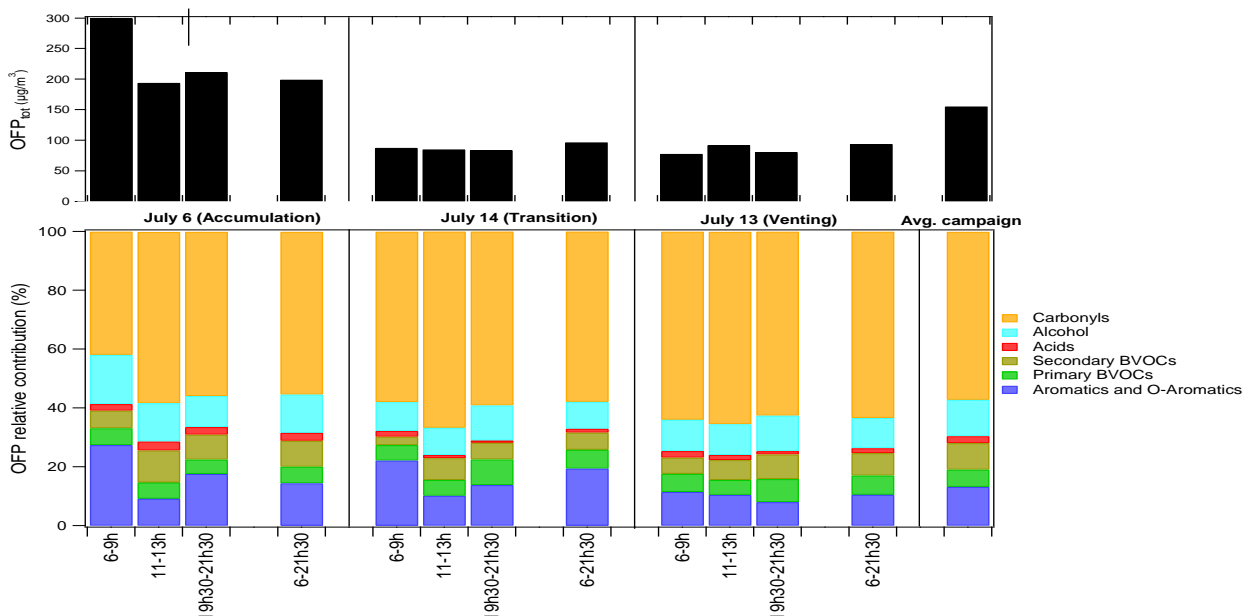
Figure S1. Ozone Formation Potential (OFP) and relative contribution of VOCs as measured by the PTR-ToF-MS (ISCIII site) to the total OFP for 3 selected days : 06/07/2016 (accumulation day), 14/07/2016 (transition day) and 13/07/2016 (venting day). For each day, we considered 3 distinct periods: Morning traffic peak (6:00-9:00 UTC), maximum insolation/biogenic VOC emissions period (11:00- 13:00 UTC), and evening traffic peak (19:30-21:30 UTC). Average daytime OFP (6:00-21:30 UTC) for each selected day as well as overall campaign average are also reported. PTR-MS measurements do not allow obtaining alkane/alkene concentrations and accordingly these are excluded in our OFP calculations.
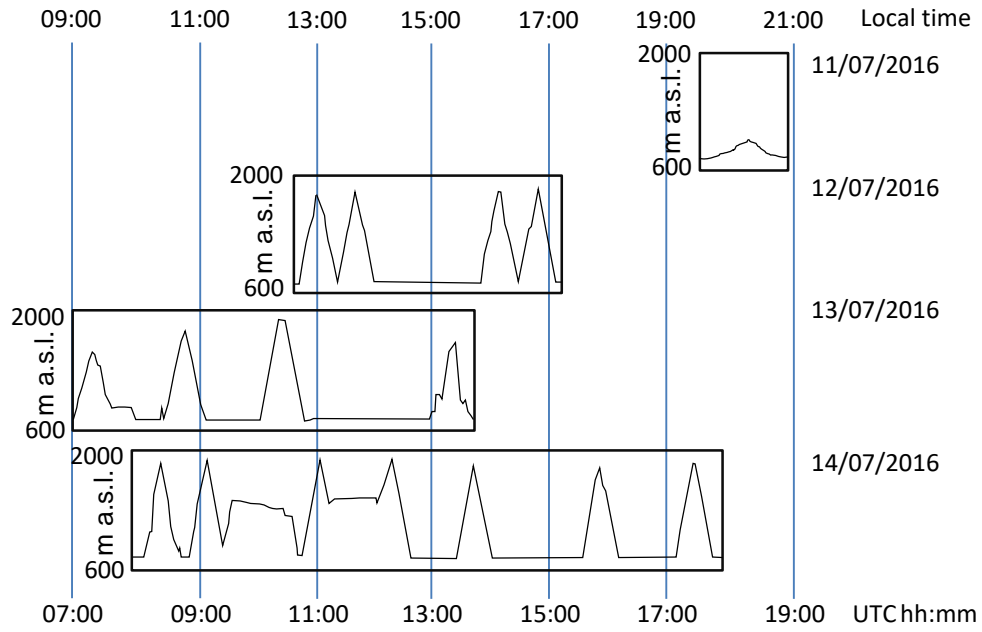
Figure S2. Timing of the vertical measurement profiles obtained during 11-14/07/2016 at Majadahonda (MJDH-RC).
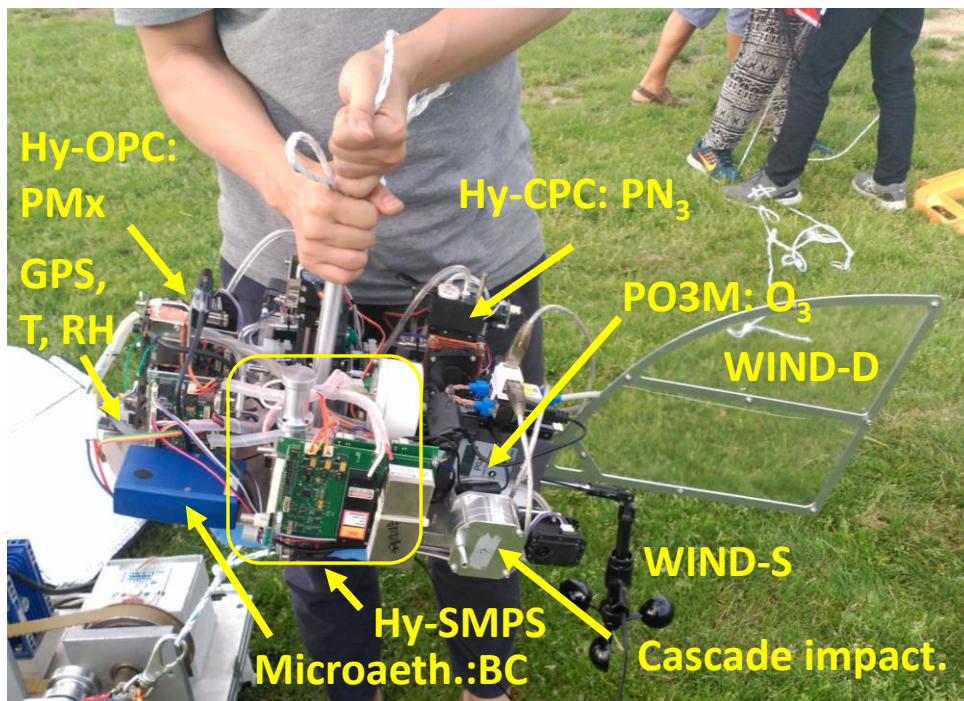
Figure S3. View of the instrumental set used for the balloon flights.
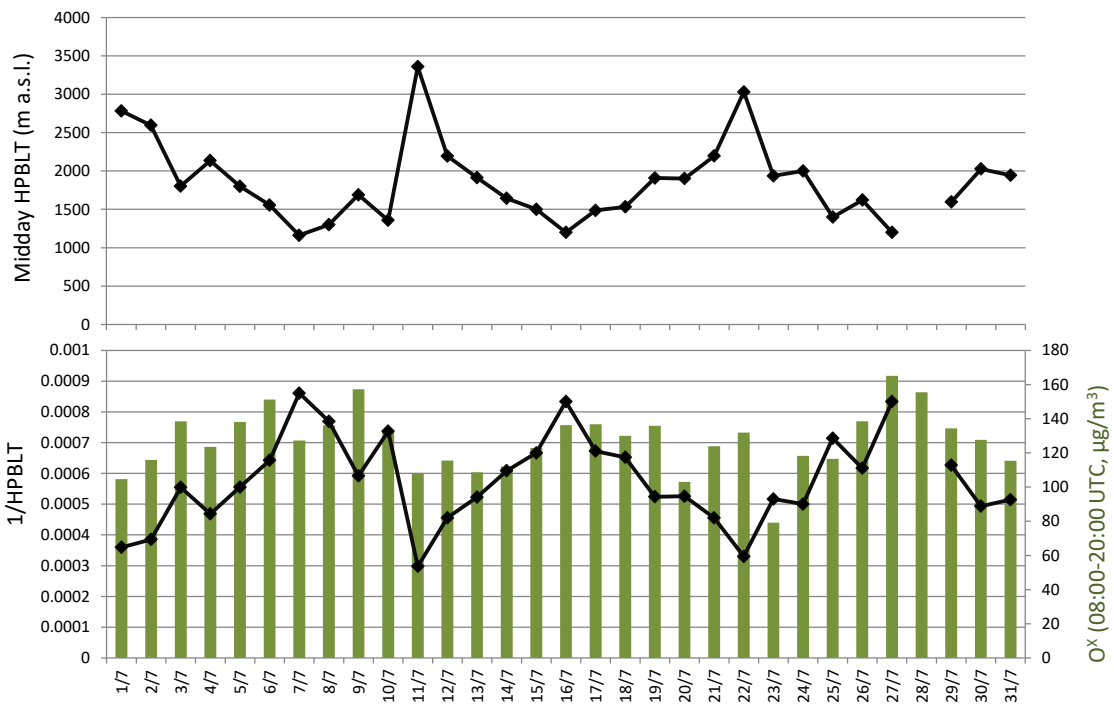
Figure S4. Top: Time series of the estimated midday height of the PBL top (HPBLT, m a.s.l.) obtained from the daily AEMET radio-soundings (using the simple parcel method) at Madrid airport for July 2016. Bottom: 1/HTPBL and average 08:00-20:00 UTC Ox concentrations at the MJDH air quality station.
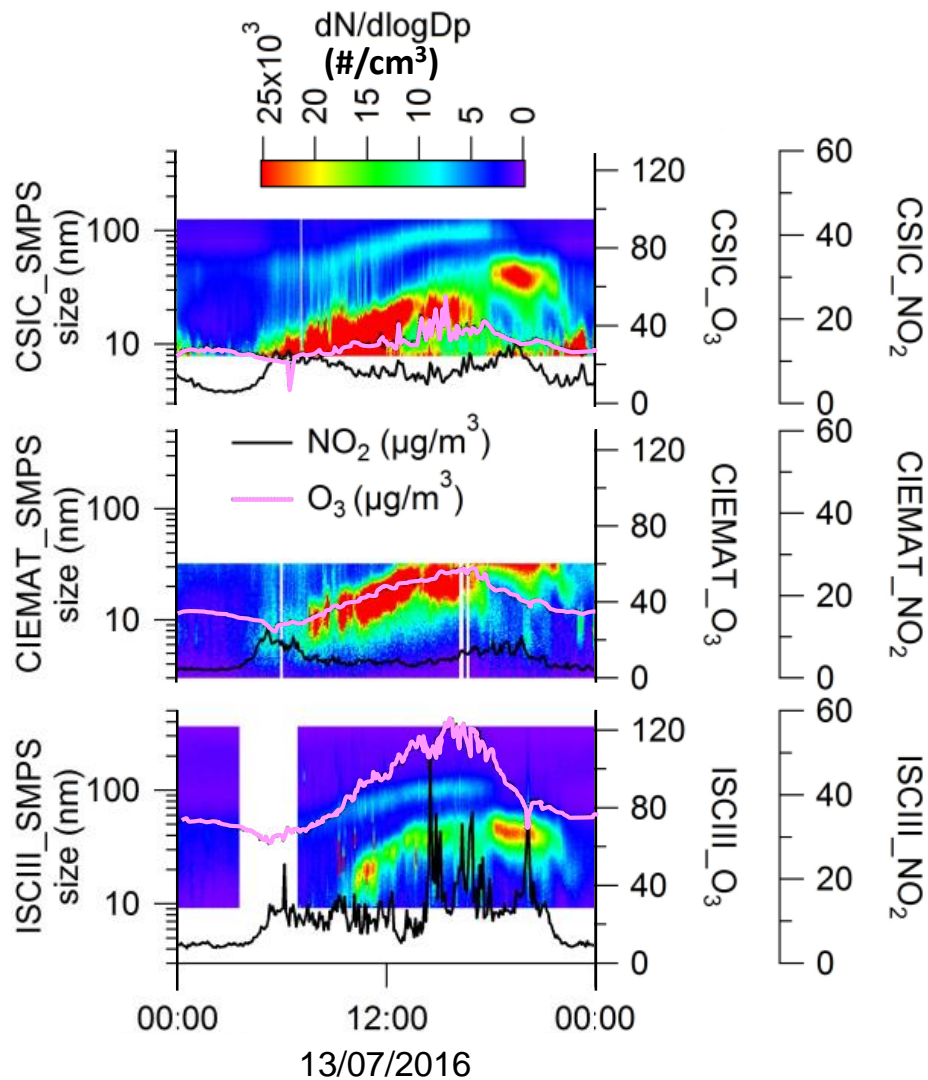
Figure S5. Example of the quasi-simultaneous occurrence of particle nucleation and growth episodes at the three supersites, with the nucleation stage coinciding with the starting of the increase of O_3 concentrations, and the growth stage with the increasing and maxima O_3 concentrations.
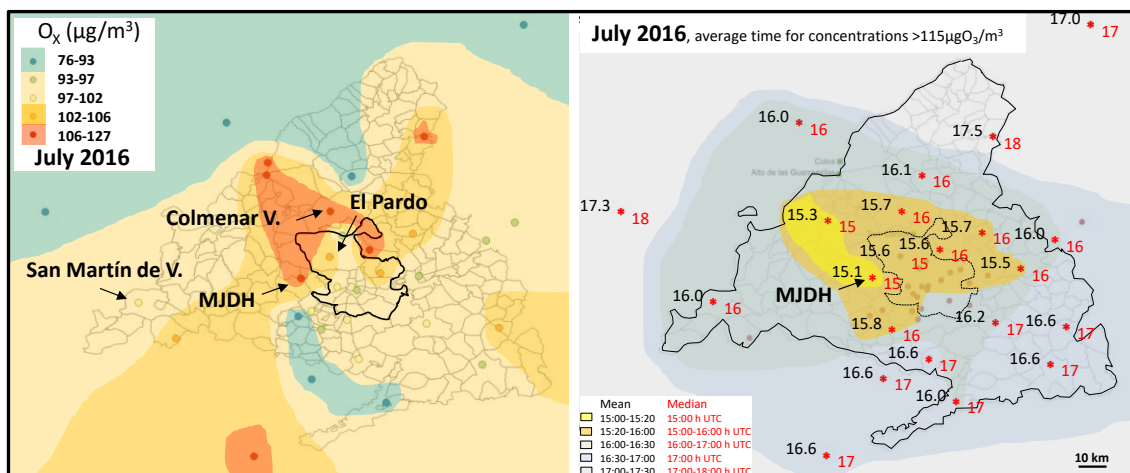
Figure S6. Left: Mean Ox (O$_3$+NO$_2$) July 2016 concentrations recorded at the monitoring sites from the Madrid air quality networks with an average concentration of NO$_2$ <25µg/m^3. Right, average time where maxima hourly concentrations >115µg/m^3 are recorded for the same period and monitoring sites. MJDH: Location of Majadahonda.